Robust Frequency and Phase Estimation for Three-Phase Power Systems Using a Bank of Kalman Filters

Zahraa Krayem Stuart, Yousef El-Laham, and Mónica F. Bugallo, *Member, IEEE*

***Abstract*—In this paper we propose a powerful frequency, phase angle, and amplitude estimation solution for an unbalanced three-phase power system based on multiple model adaptive estimation. The proposed model utilizes the existence of a conditionally linear and Gaussian substructure in the power system states by marginalizing out the frequency component. This substructure can be effectively tracked by a bank of Kalman filters where each filter employs a different angular frequency value. Compared to other Bayesian filtering schemes for estimation in three-phase power systems, the proposed model reformulation is simpler, more robust, and more accurate as validated with numerical simulations on synthetic data.**

***Index Terms*—Bayesian inference, frequency estimation, Kalman filtering, smart grids, three-phase power systems.**

I. Introduction

In the new information age, an important application area is smart energy given its impact on generation, transmission, distribution, and consumption of the smart grid. Whether we are an end user, producer, or a policy maker, controlling energy through smart devices allows for reduction of the carbon footprints to our plant, rerouting of power according to demand, enable real-time communication, and reduction of energy cost. As more distributed renewable energy power generation systems are integrated into the utility grid, accurate and efficient frequency estimation and grid synchronization strategies become a pressing issue for grid control.

A smart grid operates through a three-phase power system where the three phases correspond to a positive, negative, and neutral phase. In a balanced system, the three phases work with equal voltage magnitudes, equally separated phase angles, and a nominal frequency of $f = 60\ Hz$ (USA). Phasor measurement units (PMUs) are high-speed phase sensors that are deployed across the grid to provide interactive data and analysis of the voltage and current signals [1]. Any deficiencies in the grid can cause unbalances in the operation of the system. Magnitude, phase, and frequency steps are typical unbalances that can lead to catastrophic failures, as exhibited recently during the February 2021 Texas power outage [2]. When the system is unbalanced, no obvious relationship exists between the three phases and one must rely on estimation methods to monitor and control the grid. Estimating the state of the grid allows for estimation of both frequency and phase angles which are the most critical parameters. Only if the states are accurately estimated can balanced load/generation and grid synchronization occur. In fact, a fundamental and challenging problem is related to the distributed estimation of the aforementioned grid parameters using only partial observations, which is required for the inception of a smart utility grid [3].

A variety of approaches have been employed to solve the frequency estimation and synchronization problems (see [4] and [5] for a review). Historically, most of these methods rely on signal processing techniques, variations of the zero-crossing method, or phase-locked loop based implementations [6], [7]. These techniques do not account for noise in the power signal while methods like discrete Fourier transform assume time invariant signals which is not the case for utility grid signals [8], [9]. Least squares approaches have also been proposed, but are computationally expensive due to the need for matrix inversion at each iteration [10]. Nonparametric methods such as strictly linear, widely linear, and fuzzy adaptive filters have been extensively studied [5], [11], [12] and parametric approaches like maximum likelihood have been applied as well [13], [14].

Bayesian methods that consider a state-space model (SSM) formulation aim to estimate the posterior distribution of the grid states. In contrast to point estimates, the posterior distribution summarizes all information about the hidden states by means of a probability distribution. An SSM formulation of the grid synchronization problem was proposed in [3], allowing for the implementation of Bayesian filtering to estimate the frequency and the phase angle of the positive sequence. In this work, an extended Kalman filtering (EKF) solution was used to tackle the highly nonlinear problem by linearizing the model using a first-order Taylor approximation and then applying traditional Kalman filtering (KF). Despite the success of EKF in a variety of application areas such as navigation systems [15] and freeway traffic estimation [16], the inherently sinusoidal nature of power signals results in suboptimal performance of any linear approximations. Unscented Kalman filtering (UKF) was considered

Manuscript received March 29, 2021; revised May 18, 2021; accepted May 26, 2021. Date of publication June 8, 2021; date of current version June 24, 2021. The associate editor coordinating the review of this manuscript and approving it for publication was Dr. Xiangui Kang. *(Corresponding author: Zahraa Stuart.)*

The authors are with the Department of Electrical and Computer Engineering, Stony Brook University, Stony Brook, NY 11794 USA (e-mail: zahraa.krayem@stonybrook.edu; yousef.ellaham@stonybrook.edu; monica.bugallo@stonybrook.edu).

Digital Object Identifier 10.1109/LSP.2021.3087464

in [17], but is more computationally expensive. Particle filtering (PF) was proposed in [18] as an alternative to the KF based approaches. While PF methods have the flexibility to deal with nonlinear and non-Gaussian SSMs, they present a computational burden that is unrealistic in an online setting of grid estimation, which requires state estimates to be acquired in real-time.

In this work, we propose a novel model of the three-phase power system under voltage unbalance and frequency steps. First, by following the assumption that the grid frequency is often static and a deviation from its nominal value is an extreme event, we reformulated the model state equations by marginalizing the frequency component from the rest of the states to produce a linear SSM. This allows for simplicity in implementation through KF that guarantees optimal estimation of the conditionally linear states. Second, to combat unbalanced grid and frequency steps, we employed a bank of Kalman filters conditioned on candidate frequencies to estimate the grid's states in a manner that is similar in spirit to multiple model adaptive estimation (MMAE) [19]. Unlike EKF and UKF, the proposed scheme circumvents the use of approximation methods on the highly nonlinear three-phase power grid model and is more robust to step changes in frequency. Moreover, the proposed method can easily be parallelized and allows for a trade-off between computational complexity and accuracy. Extensive simulations show promising results of the proposed scheme when applied to three-phase power system estimation.

II. State-Space Formulation

To achieve a balanced and synchronized grid, the main obstacle is in accurately estimating the frequency and the positive phase angle of a three-phase voltage input. The voltage input of the utility grid can be modeled as follows:

$$\begin{aligned} v_{a,t} &= V_a \cos(\xi t + \varphi_a) + \epsilon_{a,t}, \\ v_{b,t} &= V_b \cos(\xi t + \varphi_b) + \epsilon_{b,t}, \\ v_{c,t} &= V_c \cos(\xi t + \varphi_c) + \epsilon_{c,t}, \end{aligned} \tag{1}$$

where t denotes the time index, v denotes the observed input, and V and φ denote the true amplitude and initial phase angle, respectively. The angular frequency is given by $\xi = (2\pi f)/f_s$, where f is the nominal grid frequency and f_s is the sampling frequency. The error vector $\boldsymbol{\epsilon}_t = [\epsilon_{a,t}, \epsilon_{b,t}, \epsilon_{c,t}]^\intercal$ is an additive noise which is assumed to be zero-mean and Gaussian distributed [20].

To simplify the analysis, we employ the Clarke transformation [21] to transform the three-phase input into the $\alpha\beta$ stationary reference frame. The transformation from the input to the $\alpha\beta$ reference frame is as follows:

$$[v_{\alpha,t}, v_{\beta,t}]^\intercal = \mathbf{T}[v_{a,t}, v_{b,t}, v_{c,t}]^\intercal, \tag{2}$$

where $\mathbf{T}$ is the Clarke transformation matrix given by

$$\mathbf{T} = \frac{2}{3}\begin{bmatrix} 1 & -\frac{1}{2} & -\frac{1}{2} \\ 0 & \frac{\sqrt{3}}{2} & -\frac{\sqrt{3}}{2} \end{bmatrix}. \tag{3}$$

The voltage signals in the $\alpha\beta$ reference frame, $v_{\alpha,t}$ and $v_{\beta,t}$, can be represented as:

$$\begin{aligned} v_{\alpha,t} &\triangleq V_\alpha \cos(\xi t + \varphi_\alpha) + \nu_{1,t}, \\ v_{\beta,t} &\triangleq V_\beta \cos(\xi t + \varphi_\beta) + \nu_{2,t}, \end{aligned} \tag{4}$$

Note that the noise vector $[\nu_{1,t}, \nu_{2,t}]^\intercal$ is also zero-mean Gaussian distributed, since the Clarke transformation is a linear transformation. From the transformed signals in (4), we formulate a grid SSM to represent all unknowns as latent states. We define the latent states as

$$\begin{aligned} x_{1,t} &= V_\alpha \cos(\xi t + \varphi_\alpha), \\ x_{2,t} &= V_\alpha \sin(\xi t + \varphi_\alpha), \\ x_{3,t} &= V_\beta \cos(\xi t + \varphi_\beta), \\ x_{4.t} &= V_\beta \sin(\xi t + \varphi_\beta), \\ x_{5,t} &= \xi, \end{aligned} \tag{5}$$

and let $\mathbf{x}_t = [x_{1,t}, x_{2,t}, x_{3,t}, x_{4,t}, x_{5,t}]^\intercal$. The state equation of the Markovian process of the latent states can be modeled as in [3]:

$$\mathbf{x}_{t+1} = f(\mathbf{x}_t, \mathbf{u}_t) = \begin{bmatrix} x_{1,t}\cos(x_{5,t}) - x_{2,t}\sin(x_{5,t}) \\ x_{1,t}\sin(x_{5,t}) + x_{2,t}\cos(x_{5,t}) \\ x_{3,t}\cos(x_{5,t}) - x_{4,t}\sin(x_{5,t}) \\ x_{3,t}\sin(x_{5,t}) + x_{4,t}\cos(x_{5,t}) \\ x_{5,t} \end{bmatrix} + \mathbf{u}_t, \tag{6}$$

where $\mathbf{u}_t \sim \mathcal{N}(\mathbf{0}, \mathbf{Q})$ is an additive multivariate Gaussian noise with covariance matrix $\mathbf{Q}$. The observation model can be written as

$$\mathbf{y}_t = \mathbf{H}\mathbf{x}_t + \boldsymbol{\nu}_t, \tag{7}$$

where $\mathbf{y}_t = [v_{\alpha,t}, v_{\beta_t}]^\intercal$ for $t = 1, \ldots, T$ and $\boldsymbol{\nu}_t \sim \mathcal{N}(\mathbf{0}, \mathbf{R})$ is multivariate Gaussian noise with covariance matrix $\mathbf{R}$ and

$$\mathbf{H} = \begin{bmatrix} 1 & 0 & 0 & 0 & 0 \\ 0 & 0 & 1 & 0 & 0 \end{bmatrix}. \tag{8}$$

Given the state and observation equations, our goal is to estimate the latent states at each time instant and then to obtain the frequency and the positive sequence phase angle. The positive sequence phase angle is obtained by the states estimates as derived in [3]:

$$\hat{\theta}_{p,t} = \arctan\left(\frac{\hat{x}_{2,t} - \hat{x}_{3,t}}{\hat{x}_{1,t} - \hat{x}_{4,t}}\right), \tag{9}$$

while the frequency can be estimated according to the state estimate of the angular frequency, i.e.,

$$\hat{f}_t = \frac{f_s \hat{x}_{5,t}}{2\pi}. \tag{10}$$

III. Proposed Solution

Our proposed solution leverages the conditionally linear substructure of the grid SSM and applies an MMAE algorithm for joint estimation of the frequency and phase in a three-phase power system. First, we partition the state vector into conditionally linear states denoted by $\mathbf{x}_t^l$ and a nonlinear state denoted by the latent frequency variable ξ:

$$\mathbf{x}_t = \begin{bmatrix} \mathbf{x}_t^l \\ \xi \end{bmatrix}, \tag{11}$$

where $\mathbf{x}_t^l = [x_{1,t}, x_{2,t}, x_{3,t}, x_{4,t}]^\intercal$. Our goal is to sequentially estimate the posterior distribution of the grid states and the angular frequency, i.e.,

$$p(\mathbf{x}_t^l, \xi|\mathbf{y}_{1:t}) = p(\mathbf{x}_t^l|\xi, \mathbf{y}_{1:t})p(\xi|\mathbf{y}_{1:t}). \tag{12}$$

As shown in (12) the posterior can be broken into two parts: the marginal posterior distribution of the angular frequency $p(\xi|\mathbf{y}_{1:t})$ and the conditional posterior distribution of the voltage states $p(\mathbf{x}_t^l|\xi, \mathbf{y}_{1:t})$. Rather than try to obtain the true posterior distribution over ξ, we will resort to a discrete approximation by only considering M possible candidate values for the angular frequency.

To initialize the algorithm, a set of M candidate values of the angular frequency will be proposed by drawing samples from a prior distribution:

$$\xi^{(m)} \sim p(\xi), \quad m = 1, \ldots, M. \tag{13}$$

The prior distribution should be chosen so that the drawn samples are reasonable values for the angular frequency. For instance, a uniform prior centered at $\xi = \frac{2\pi f}{fs}$, with nominal frequency $f = 60\ Hz$, is a suitable choice. Each of these proposed values is fed into a different Kalman filter, which updates the estimate of linear states conditioned on the candidate angular frequency. In other words, the mth KF algorithm is responsible for tracking $p(\mathbf{x}_t^l|\xi^{(m)}, \mathbf{y}_{1:t})$, which assumes that the angular frequency value is fixed to $\xi^{(m)}$.

After the KF step of the MMAE algorithm, we proceed to weighting the estimates from each of the Kalman filters. According to the theory of Bayesian model averaging, if we assume that there are only M possible angular frequencies $\{\xi^{(m)}\}_{m=1}^M$, the posterior over states through marginalization of those frequencies is given by

$$p(\mathbf{x}_t^l|\mathbf{y}_{1:t}) = \sum_{m=1}^{M} w_t^{(m)} p(\mathbf{x}_t^l|\xi^{(m)}, \mathbf{y}_{1:t}), \tag{14}$$

where the weight $w_t^{(m)} = p(\xi^{(m)}|\mathbf{y}_{1:t})$. The weights can be expressed as follows by applying Bayes' theorem:

$$w_t^{(m)} \propto p(\mathbf{y}_{1:t}|\xi^{(m)})p(\xi^{(m)}), \tag{15}$$

where $p(\mathbf{y}_{1:t}|\xi^{(m)})$ is the marginal likelihood of the mth Kalman filter at time t. KF provides us with a mechanism for computing this marginal likelihood. In particular, we can establish the following recursive formula for computing the marginal likelihood:

$$\begin{aligned} p(\mathbf{y}_{1:t}|\xi) &= p(\mathbf{y}_{1:t-1}|\xi)p(\mathbf{y}_t|\mathbf{y}_{1:t-1}, \xi) \\ &= p(\mathbf{y}_{1:t-1}|\xi) \int p(\mathbf{y}_t|\mathbf{x}_t^l, \xi)p(\mathbf{x}_t^l|\xi, \mathbf{y}_{1:t-1})d\mathbf{x}_t^l \\ &= p(\mathbf{y}_{1:t-1}|\xi)\mathcal{N}(\mathbf{y}_t|\mathbf{H}\mathbf{x}_{t|t-1}, \mathbf{S}_t). \end{aligned} \tag{16}$$

Using the marginal likelihood, the set of weights $\{w_t^{(m)}\}_{m=1}^M$ are computed according to (15). Finally, the estimate of the linear states, their covariance matrices, and the candidate angular frequency values are fused to obtain the final estimates of $\mathbf{x}_t^l$, $\mathbf{P}_t$, and ξ at time t, respectively as shown in step 6 of Table I. The proposed algorithm is summarized in Table I and is henceforth referred to as MMAE for three-phase power systems (MMAE-TPPS). The implementation in Table I also includes a forgetting factor parameter α, which controls the influence of the observation history in the computation of the model weights. Using a forgetting factor is equivalent to using a biased estimate of the marginal likelihood at time t that tempers the value the marginal likelihood at time $t-1$:

$$p(\mathbf{y}_{1:t}|\xi) \approx p(\mathbf{y}_{1:t-1}|\xi)^{\alpha}\mathcal{N}(\mathbf{y}_t|\mathbf{H}\mathbf{x}_{t|t-1}, \mathbf{S}_t). \tag{17}$$

TABLE I
T IS TIME LENGTH AND M IS THE NUMBER OF GRID POINTS

Algorithm: MMAE-TPPS

1. **Initialization:**
 a. $\xi_0^{(m)} \sim p(\xi_0), \quad m = 1, \ldots, M$
 b. Set $w^{(m)} = \frac{1}{M}, \quad m = 1, \ldots, M$
 c. Initialize $\mathbf{x}_0^l$ and $\mathbf{P}_0$
2. **For:** $t = 1, ..., T$
3. **For:** $m = 1, ..., M$
 a. Predict the prior state estimate and covariance,
 $\mathbf{x}_{t|t-1}^{l(m)} = \mathbf{F}\mathbf{x}_{t-1}^l$
 $\mathbf{P}_{t|t-1}^{(m)} = \mathbf{F}\mathbf{P}_{t-1}\mathbf{F}^{\mathsf{T}} + \mathbf{Q}$
 b. Calculate the innovation and its covariance,
 $\mathbf{z}^{(m)} = \mathbf{y}_t - \mathbf{H}\mathbf{x}_{t|t-1}^{l(m)}$
 $\mathbf{S}^{(m)} = \mathbf{H}\mathbf{P}_{t|t-1}^{(m)}\mathbf{H}^{\mathsf{T}} + \sigma_y^2\mathbb{I}_2$
 c. Compute the optimal Kalman gain,
 $\mathbf{K}^{(m)} = \mathbf{P}_{t|t-1}^{(m)}\mathbf{H}^{\mathsf{T}}\{\mathbf{S}^{(m)}\}^{-1}$
 d. Update the posterior state estimate and covariance,
 $\mathbf{x}_{t|t}^{l(m)} = \mathbf{x}_{t|t-1}^{l(m)} + \mathbf{K}^{(m)}\mathbf{z}^{(m)}$
 $\mathbf{P}_{t|t}^{(m)} = (\mathbb{I}_2 - \mathbf{K}^{(m)}\mathbf{H})\mathbf{P}_{t|t-1}^{(m)}$
 e. Update the log-likelihood of each ξ model,
 $l_{log}^{(m)} = \alpha \times l_{log}^{(m)} - \frac{1}{2}\Big[\mathbf{z}^{(m)T}\{\mathbf{S}^{(m)}\}^{-1}\mathbf{z}^{(m)}$
 $+\log(|\mathbf{S}^{(m)}|) + 2\log(2\pi)\Big]$
4. Convert the log-likelihood to the likelihood,
 $l^{(m)} = \exp(l_{log}^{(m)} - \max(l_{log}^{(m)})), \quad m = 1.., M$
5. Normalize the likelihood,
 $w^{(m)} = l^{(m)} / \sum_{i=1}^{M} l^{(i)}, \quad m = 1, ..., M$
6. Weighted sum the estimates and covariances of models,
 $\mathbf{x}_t^l = \sum_{m=1}^{M} w^{(m)}\mathbf{x}_{t|t}^{l\ (m)}$
 $\mathbf{P}_t = \sum_{m=1}^{M} w^{(m)}\Big[\mathbf{P}_{t|t}^{(m)} + (\mathbf{x}_{t|t}^{l\ (m)} - \mathbf{x}_t^l)(\mathbf{x}_{t|t}^{l\ (m)} - \mathbf{x}_t^l)^{\mathsf{T}}\Big]$
 $\xi_t = \sum_{m=1}^{M} w^{(m)}\xi_t^{(m)}$
7. **Return:** $\mathbf{x}_1^l, \mathbf{x}_2^l, \ldots, \mathbf{x}_T^l$ & $\xi_1, \xi_2, \ldots, \xi_T$

IV. SIMULATIONS

In this section we describe the simulations carried out to demonstrate the performance of the proposed solution in estimating the frequency, positive phase angle, and grid states. We also provide a comparison to EKF and UKF, where the results are averaged over 500 Monte Carlo simulations. The simulated data is generated under both voltage and frequency imbalances over a period of 1 s at the rate of $f_s = 500\ Hz$ with $f = 60\ Hz$ as a nominal frequency. The observation noise is assumed to be $\mathbf{R} = \sigma_r^2\mathbb{I}_2$ with $\sigma_r^2 = 10^{-5}$, the average value of observation noise in PMUs [20]. Voltages are simulated with a uniform prior centered at 110v for the voltage imbalance scenario with process noise

$$\mathbf{Q} = \begin{bmatrix} \sigma_q^2\mathbb{I}_4 & 0 \\ 0 & \sigma_\xi^2 \end{bmatrix}, \tag{18}$$

where $\sigma_q^2 = 10^{-4}$, $\sigma_\xi^2 = 10^{-12}$. We test the proposed solution under a double frequency abruption introduced at 0.4 s from

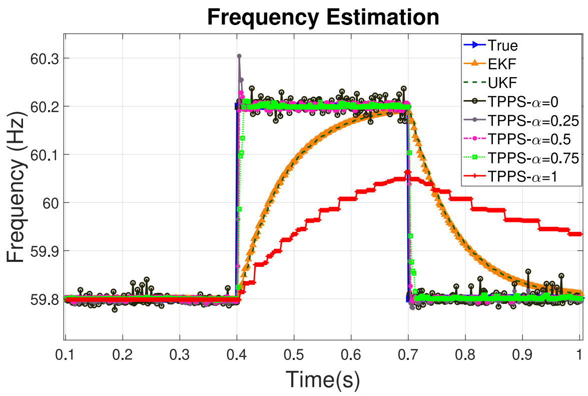

Fig. 1. Frequency tracking for two-step frequency abrutpion.

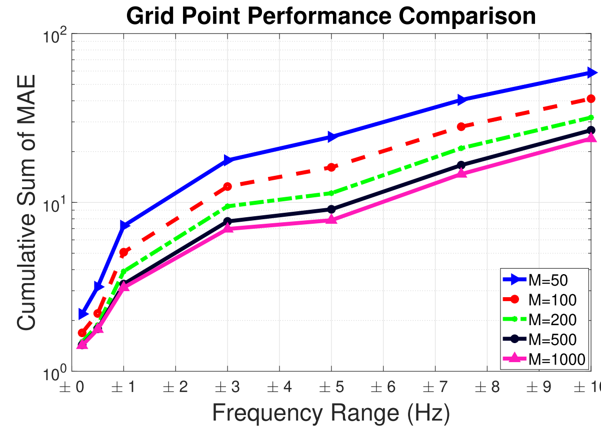

Fig. 2. Grid point performance comparison.

TABLE II
AVERAGE MAE OVER 500 SIMULATIONS

Average MAE						
	1 Step Frequency Abruption			**2 Step Frequency Abruption**		
	ξ	θ_p	$\mathbf{x}^l$	ξ	θ_p	$\mathbf{x}^l$
TPPS($\alpha = 0$)	0.0649	0.0379	5.2913	0.0743	0.0406	5.6130
TPPS($\alpha = 0.25$)	0.0447	**0.0295**	**4.4349**	0.0542	**0.0314**	**4.6065**
TPPS($\alpha = 0.5$)	0.0430	0.0317	4.6949	**0.0518**	0.0335	4.8574
TPPS($\alpha = 0.75$)	**0.0406**	0.0327	4.7248	0.0549	0.0385	5.3377
TPPS($\alpha = 1$)	0.6398	0.5243	60.5642	0.8113	0.6621	76.0848
EKF	0.2036	0.1695	20.2616	0.3967	0.3190	36.9042
UKF	0.2082	0.3751	47.4822	0.4062	0.7152	88.3419

59.8 Hz to 60.2 Hz and another at 0.7 s from 60.2 Hz to 59.8 Hz. A faster emergency response due to steep frequency changes is needed with more distributed RES integrated into the utility grid [22], [23]. The number of grid points used in the proposed solution is $M = 100$ where $\xi^{(m)}$ values are uniformly sampled from $[\frac{2\pi(59.5)}{fs}, \frac{2\pi(60.5)}{fs}]$. We remark that a ± 0.4 Hz change in nominal frequency is commonly catastrophic and requires attention [24].

To show the effectiveness of the proposed solution in the presence of a frequency abruption, we test the MMAE-TPPS scheme with different forgetting factors $\alpha \in \{0, 0.25, 0.5, 0.75, 1\}$. As shown in Fig. 1, MMAE-TPPS is able to track the frequency abruption for most values α, but struggles to track the frequency with $\alpha = 1$. Recall that the forgetting factor is used to discount the importance of the observation history and biases the marginal likelihood estimate. It pays off to bias the marginal likelihood estimate as shown in (17) especially in the presence of frequency steps. The peakiness of the likelihood, $\sigma_r^2 = 10^{-5}$, explains why our method struggles with a $\alpha = 1$, since old data is not neglected. In contrast, with a smaller forgetting factor value, newer data has more influence in the estimation results. The estimates fluctuate more around the ground truth, but are more robust to instantaneous frequency changes.

To evaluate the performance of our proposed solution as compared to EKF and UKF, we select a forgetting factor of $\alpha = 0.75$, where there is a good trade-off between the robustness to frequency changes and the accuracy in the estimation. The rate of convergence and tractability of the estimates are very critical in three-phase voltage power systems. The superior performance of the proposed solution over EKF and UKF can clearly be observed from the curves presented in Fig. 1. This shows that the MMAE-TPPS is more robust and produces a more accurate estimation under an unbalanced power grid.

The number of grid points M can be chosen to balance a trade-off between computational complexity and accuracy in the estimations. To account for the possibility of a bigger frequency abruptions, a wider frequency range is considered when defining the uniform prior over ξ. Figure 2 shows the performance comparison of different frequency priors $f \pm \{0.2, 0.5, 1, 3, 5, 7.5, 10\}Hz$ with different grid points $M \in \{50, 100, 200, 500, 1000\}$. As expected, the results indicate the need for larger grid point M for wider frequency range and abruption to maintain a good accuracy in estimation. The computational complexity of a single KF is similar to that of the EKF, while UKF requires an order of magnitude higher effort [25], [26]. We note that the computational complexity of the proposed solution can be reduced by leveraging distributed computing resources, since the algorithm can easily be parallelized into M Kalman filters.

We summarize the mean absolute error (MAE) as a performance metric in Table II. MAE is used because it is more robust to outliers and sudden abruption. MMAE-TPPS with forgetting factor of $\alpha \in \{0.25, 0.5, 0.75\}$ produces similar results in terms of MAE. We can see that the MMAE-TPPS has a lower average MAE at $\alpha < 1$ than both EKF and UKF for frequency, positive phase angle, and linear states estimation and is less sensitive to initialization.

V. CONCLUSIONS

In this work, we proposed a novel model reformulation for estimation in three-phase voltage power system applications. By utilizing the conditionally linear SSM, we were able to optimally estimate the states of the system by using a bank of parallel Kalman filters based on MMAE. In case of different unbalances, one might need a different model formulation that does not utilize the conditionally linear and Gaussian substructure of the states. Simulation results indicated that the proposed solution outperforms other Bayesian filtering schemes under power system imbalances.

REFERENCES

[1] E. Kabalci and Y. Kabalci, *Smart Grids and Their Communication Systems*, Berlin, Germany: Springer, 2019.

[2] B. Magness, "Review of Feb. 2021 Extreme Cold Weather Event - Ercot Presentation," 2021. [Online]. Available: http://www.ercot.com/content/wcm/key_documents_lists/225373/2.2_REVISED_ERCOT_Presentation.pdf

[3] M. Sun and Z. Sahinoglu, "Extended Kalman filter based grid synchronization in the presence of voltage unbalance for smart grid," in *Proc. Innovat. Smart Grid Technol. (ISGT)*, 2011, pp. 1–4.

[4] A. Timbus, M. Liserre, R. Teodorescu, and F. Blaabjerg, "Synchronization methods for three phase distributed power generation systems-An overview and evaluation," in *Proc. IEEE 36th Power Electron. Specialists Conf.*, 2005, pp. 2474–2481.

[5] E. C. Mengüç and N. Acir, "Frequency estimation methods for smart grid systems," in *Smart Grids Their Communication Systems*, pp. 171–195. Berlin, Germany: Springer, 2019.

[6] C. T. Nguyen and K. Srinivasan, "A new technique for rapid tracking of frequency deviations based on level crossings," *IEEE Trans. Power App. Syst.*, vol. PAS-103, no. 8, pp. 2230–2236, Aug. 1984.

[7] M. Karimi-Ghartemani and M. R. Iravani, "A nonlinear adaptive filter for online signal analysis in power systems: Applications," *IEEE Trans. Power Del.*, vol. 17, no. 2, pp. 617–622, Apr. 2002.

[8] C. Yu, "A discrete Fourier transform-based adaptive mimic phasor estimator for distance relaying applications," *IEEE Trans. Power Del.*, vol. 21, no. 4, pp. 1836–1846, Oct. 2006.

[9] H. Wen, S. Guo, Z. Teng, F. Li, and Y. Yang, "Frequency estimation of distorted and noisy signals in power systems by FFT-based approach," *IEEE Trans. Power Syst.*, vol. 29, no. 2, pp. 765–774, Mar. 2014.

[10] D. Lee, S. Kang, and S. Nam, "Modified dynamic phasor estimation algorithm for the transient signals of distributed generators," *IEEE Trans. Smart Grid*, vol. 4, no. 1, pp. 419–424, Mar. 2013.

[11] Y. Xia and D. P. Mandic, "Widely linear adaptive frequency estimation of unbalanced three-phase power systems," *IEEE Trans. Instrum. Meas.*, vol. 61, no. 1, pp. 74–83, Jan. 2012.

[12] S. Nanda, P. K. Dash, T. Chakravorti, and S. Hasan, "A quadratic polynomial signal model and fuzzy adaptive filter for frequency and parameter estimation of nonstationary power signals," *Measurement*, vol. 87, pp. 274–293, 2016.

[13] Y. Xia, S. Kanna, and D. P. Mandic, "Maximum likelihood parameter estimation of unbalanced three-phase power signals," *IEEE Trans. Instrum. Meas.*, vol. 67, no. 3, pp. 569–581, Mar. 2018.

[14] V. Choqueuse, E. Elbouchikhi, and M. Benbouzid, "Maximum likelihood frequency estimation in smart grid applications," in *Proc. IEEE 24th Int. Symp. Ind. Electron. (ISIE)*, 2015, pp. 1339–1344.

[15] E. Wan, "Sigma-point filters: An overview with applications to integrated navigation and vision assisted control," in *Proc. IEEE Nonlinear Stat. Signal Process. Workshop*, 2006, pp. 201–202.

[16] Y. Wang and M. Papageorgiou, "Real-time freeway traffic state estimation based on extended Kalman filter: A general approach," *Transp. Res. Part B: Methodological*, vol. 39, no. 2, pp. 141–167, 2005.

[17] P. Regulski and V. Terzija, "Estimation of frequency and fundamental power components using an unscented Kalman filter," *IEEE Trans. Instrum. Meas.*, vol. 61, no. 4, pp. 952–962, Apr. 2012.

[18] J. Zhu, Z. Shi, H. Liang, R. Lu, and X. Shen, "Particle filter based grid synchronization with voltage unbalance and frequency variation in smart grid," in *Proc. IEEE Int. Conf. Wireless Commun. Signal Process. (WCSP)*, 2013, pp. 1–6.

[19] P. S. Maybeck and P. D. Hanlon, "Performance enhancement of a multiple model adaptive estimator," *IEEE Trans. Aerosp. Electron. Syst.*, vol. 31, no. 4, pp. 1240–1254, Oct. 1995.

[20] M. Brown, M. Biswal, S. Brahma, S. J. Ranade, and H. Cao, "Characterizing and quantifying noise in PMU data," in *Proc. IEEE Power Energy Soc. Gen. Meet. (PESGM)*, 2016, pp. 1–5.

[21] D. P. Mandic, S. Kanna, Y. Xia, A. Moniri, A. Junyent-Ferre, and A. G. Constantinides, "A data analytics perspective of power grid analysis-Part 1: The clarke and related transforms," *IEEE Signal Process. Mag.*, vol. 36, no. 2, pp. 110–116, Mar. 2019.

[22] Y. Yap, C. Sarimuthu, and J. Lim, "Virtual inertia-based inverters for mitigating frequency instability in grid-connected renewable energy system: A review," *Appl. Sci.*, vol. 9, no. 24, 2019, Art. no. 5300.

[23] S. Ratnam, K. Palanisamy, and G. Yang, "Future low-inertia power systems: Requirements, issues, and solutions-A review," *Renewable Sustain. Energy Rev.*, vol. 124, 2020, Art. no. 109773.

[24] S. Hassan, H. Sajjad, and M. M. Rahman, "Power imbalance detection in smart grid via grid frequency deviations: A hidden Markov model based approach," in *Proc. IEEE 88th Veh. Technol. Conf. (VTC-Fall)*, 2018, pp. 1–5.

[25] D. Simon, "A comparison of filtering approaches for aircraft engine health estimation," *Aerosp. Sci. Technol.*, vol. 12, no. 4, pp. 276–284, 2008.

[26] B. Zhang, H. Chu, T. Sun, H. Jia, L. Guo, and Y. Zhang, "Error prediction for SINS/GPS after GPS outage based on hybrid KF-UKF," *Math. Problems Eng.*, vol. 2015, 2015, Art. no. 239426.